Accelerating antibiotic discovery by leveraging machine learning models: Application to identify novel inorganic complexes

Miroslava Nedyalkova,[1] Gözde Demirci,[1] Youri Cortat,[1] Kevin Schindler,[1] Fatlinda Rhamani,[1] Aleksandar Pavic,[2] Fabio Zobi,[1*] and Marco Lattuada[1*]

[1]Department of Chemistry, Fribourg University, Chemin Du Musée 9, 1700 Fribourg, Switzerland

[2]Institute of Molecular Genetics and Genetic Engineering, University of Belgrade, Vojvode Stepe 444a, 11042 Belgrade, Serbia

KEYWORDS: Antibiotic-resistant, machine-learning, minimum inhibitory concentration, metal complexes

ABSTRACT: New antibiotics are required to combat the emergence of drug-resistant bacteria. *S. aureus* is a Gram-positive pathogen that often displays multidrug resistance. Through conventional screening approaches, the discovery of new antibiotics against *S. aureus* has proven to be challenging. Molecular property prediction of novel antibiotics candidates by machine-learning (ML) methods has increased the rate at which such molecules are identified. The bottleneck of the existing approaches relies on the structure similarities for the existing antibiotics. Then the question about discovering and developing new unconventional antibiotic classes has challenged preconceptions about the scope and applicability of the existing methods. Herein, we developed an ML approach that predicts the minimum inhibitory concentration (MIC) of Re-complexes towards two *S. aureus* strains (ATCC 43300 - MRSA and ATCC 25923 - MSSA). In our framework, we tailored a Multi-layer Perceptron (MLP) by inherently accounting for the structure features of the Re- complexes to develop a prediction model for antimicrobial activity assessment. Although our approach is demonstrated with a specific example based on the rhenium carbonyl complexes, the predictive model can be readily adapted to other candidate metal complexes. The developed model emphasizes the application of machine learning in the *de novo* design of a novel generation of antibiotic molecules with targeted activity against a challenging pathogen.

INTRODUCTION

It has been recognized that the emergence of antibiotic-resistant microbes represents a "clear and present danger" with a global impact, and, therefore, an effective response should be facilitated by adopting a novel approach for the *de-novo* design of novel classes of microbicides. As much as one-third of Healthcare-Associated Infection (HAI) cases can be attributed to environmental surfaces, particularly hospital “high touch” surfaces (e.g., bed rails, machine buttons, and equipment). The number of HAI cases reported in hospitals in the United States is estimated to be 1.7 million annually, resulting in 99,000 deaths and an estimated $20 billion in healthcare costs. Organometallic complexes, especially rhenium-based complexes [1–8], have recently emerged as potent antibacterial agents and hold promise thanks to the flexibility of their chemistry that allows one to change their structure and the nature of their ligands. Their mechanism of action is not fully understood, but current evidence points to the bacterial membranes as the target of compounds. [9–119–11] In addition to the lack of information about how these antimicrobial agents behave, the molecular features contributing to their bactericidal effectiveness are also unknown. The development of novel approaches to antibiotic discovery is required in order to increase the rate at which new antibiotics are discovered and reduce the associated costs of lead identification in early preclinical testing. As a result of recent advances in machine learning (ML) the field is now able to predict a plethora of molecular properties, and to apply the same to identify new antibiotic structural classes. [12–16]

Exploring vast chemical spaces outside the reach of current experimental approaches is possible by adopting methodologies that enable early drug discovery in silico. ML could offer an alternative approach to streamline the development process of de novo antibiotics by identifying the key motif in the molecular structure associated with antibiotic activity. The application of ML to drug discovery, specifically antibiotic discovery, has been greatly facilitated by the public availability of empirical datasets.[17-20] Antibacterial screening approaches still do not have efficient tools and strategies for rapidly increasing the number of new chemotypes. Implementing the ML methods for novel compounds acting against Gram-negative bacteria is scarcely used. One example is the Open Antimicrobial Drug Discovery (CO-ADD) for metal-containing compounds with antimicrobial activity. [21-22]

ML-guided approach based on descriptor space search and selection has already been used to predict antimicrobial activity. [23–26] The way of representing molecules is a crucial step. Numeric vectors consisting of molecular descriptor values (features) have already been utilized before the widespread applicability of ML in QSAR (quantitative structure−activity relationship) modeling. Molecular graph networks are another way of describing molecules where each atom is represented as a node, and each bond between the atoms is represented as an edge. There is a close relationship between ML models and molecular representations. Depending on how the chemical structures are presented, the chemical space can be defined as the union of all possible chemical compounds that can be used to find new antibiotic candidates that resemble existing ones.

Herein, we preset an application of the ML approach for the prediction of the antibacterial activity of new antibiotic candidates based on Re-metal complexes towards two *S. aureus* strains (namely ATCC 43300, MRSA and ATCC 25923, MSSA), using molecular descriptors and neural network architectures. Our framework provides a rapid method for developing a model able to predict minimum inhibitory concentrations (MIC) of the metal complexes. It consists of the following elements: (1) molecular representation based on the structure of the complexes, (2) feature reduction space, (3) ML algorithm, and (4) molecular descriptor specificity analysis (featuring importance scores). By leveraging the physicochemical properties captured by the molecular structures of 119 Re-complexes, measured data points (minimum inhibitory concentration) towards the activity of *S. aureus* ATCC 43300 and *S. aureus* ATCC 25923 strains were used for the antimicrobial activity prediction of previously untested complexes.

Results and Discussion

Synthesis of metal complexes

A dataset of 119 $Re(CO)_3$ complexes was compiled for this work. Of these, 20 complexes, not previously evaluated for their antibiotic activity, were synthesized and used as the validation set for the model (Figure 1). Complexes shown in Figure 1 were prepared according to well-established procedures employed in the chemistry of this metal core. $[Re(CO)_3(NN)X]$ species (where NN = diimine ligand and X = halide; Br or Cl) were obtained by reacting commercially available $Re(CO)_5X$ with one equivalent of NN in refluxing toluene. Upon cooling, the desired compounds precipitate and are then filtered and washed with a cold solvent to yield the molecules with a purity ≥ 95%. Pyridine (py) and clotrimazole (ctz) derivatives of the compounds were prepared by reaction of $[Re(CO)_3(NN)X]$ with AgOTf in the presence of py or ctz, followed by precipitation and HPLC purification. Characterization of the new compounds is given in SI.

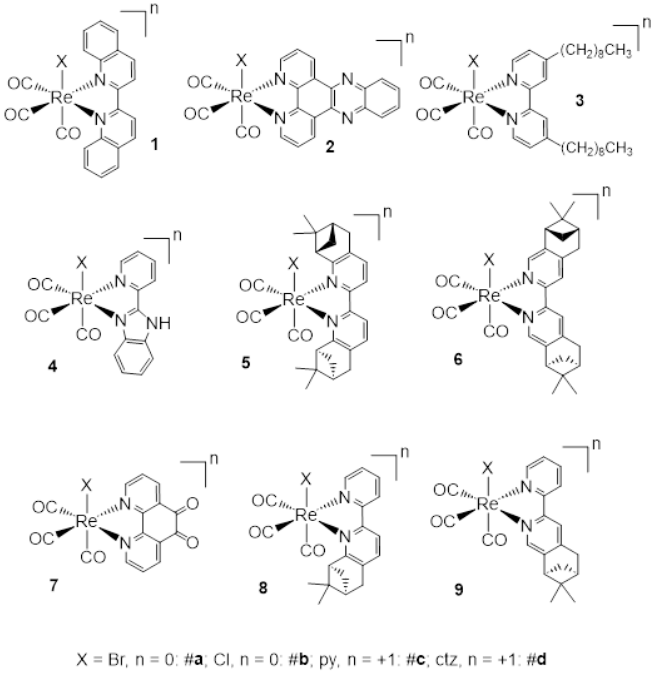

Figure 1. Structures of validation complexes tested for antimicrobial activity against *S. aureus* ATCC 25923 (MSSA) and *S. aureus* ATCC 43300 (MRSA) strains.

Predictive model: integration for Re-complexes tested for antimicrobial activity.

The pipeline for leveraging the prediction model based on antimicrobial data is presented in Figure 2. Using the MLP, we predicted the antimicrobial activity, quantified in the MIC values Re-complexes. We trained the MLP architecture on the whole set. The obtained scores were computed based on the validation set and showed model performs by comparing the model's predictions to the experimental validation values. The prediction performance was evaluated using the following parameters: accuracy, precision, and recall. Accuracy estimates how often the model predictions were correct. As such, it is the ratio of the true cases to all the cases, defined as (TP + TN) / (TP + FP + TN + FN) where TP is the number of true positives, FP is the number of false positives, TN is the number of true negatives, FN is the number of false negatives. The set of labels predicted for a sample must match the corresponding labels in the validation set. Precision indicates how often the model predicted the sample to be positive when true. It is defined as the ratio of the True Positive to the predicted positive cases. The precision is equal to TP / (TP + FP). It is intuitively the ability of the classifier not to label as positive a sample that is negative. Recall quantifies the number of positive predictions made from all positive cases in the dataset, equal to TP / (TP + FN). The classifier intuitively can find all the positive samples. The obtained scores are shown in Table 1 and Figure 3.

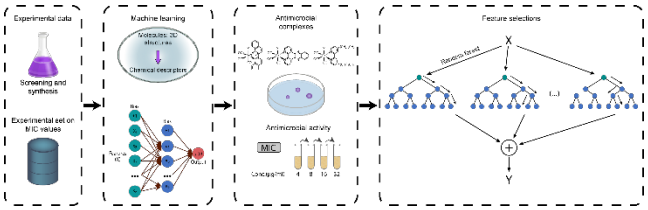

Figure 2. Schematic representation of the workflow. We started from experimentally obtained data to compile the input matrix for training and testing the model. For validating the model was used the new synthesized Re-complexes. The descriptors were extracted from the AlvaDesc software, and the MLP was used to predict the antimicrobial activity. The last box: scoring the molecular features by recursive feature elimination based on bootstrap-aggregated decision trees.

Table 1. Model prediction performance evaluated by Accuracy, Precision, and Recall criteria.

Target	Accuracy	Precision	Recall
MRSA[a] – MIC [b] 4	0.9	0.85	0.92
MRSA - MIC 8	0.83	0.78	0.93
MRSA - MIC 16	0.87	0.81	1
MRSA - MIC 32	0.9	0.94	0.89
MSSA[c] - MIC 4	0.8	0.64	0.9
MSSA - MIC 8	0.83	0.75	0.92
MSSA - MIC 16	0.87	0.84	0.94
MSSA - MIC 32	0.73	0.74	0.82

[a] MRSA refers to *S. aureus* ATCC 43300 strain. [b] MIC # indicates the target minimum inhibitory concentration in μM. [c] MSSA refers to *S. aureus* ATCC 25923 strain.

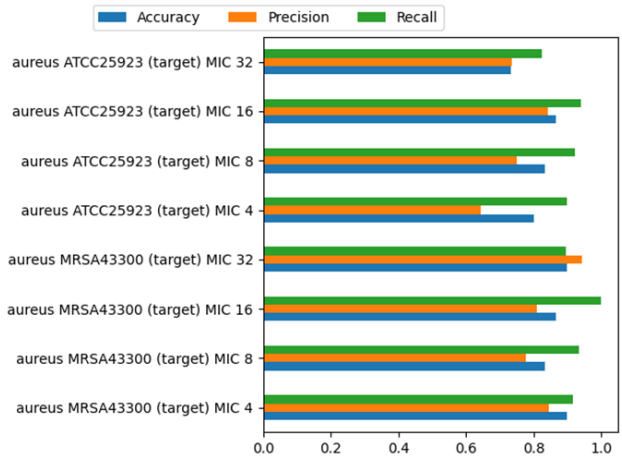

Figure 3. Model prediction performance evaluated by Accuracy, Precision, and Recall criteria. For all these scores, the best value is 1, and the worst value is 0.

In practical terms, the model can predict, with overall good accuracy, whether a metal complex may be active against the MRSA *S. aureus* strain. Indeed, a good agreement between predicted and experimental MIC values is found when considering the methicillin-resistant *S. aureus* ATCC 43300. The complete statistical metrics are presented in Table S1 for the validation set. In this case, in 14 out of 20 instances (Table 2), the model correctly predicted whether a metal complex showed no activity (MIC > 32 ug/mL, 7 out of 10 experimentally inactive compounds) or if a complex had potential antibacterial activity (MIC < 32 ug/mL, 7 out of 10 experimentally active compounds). In this latter case, in 6 out of 7 instances, the MIC value was correctly predicted within 2x of the experimentally determined MIC value. When considering the wild-type *S. aureus* ATCC 25923 (MSSA) strain, the model revealed more limitations. However, in the case of experimentally active molecules, not only the model always correctly identified these complexes (8 out of 8 instances within 2x the experimentally determined MIC value), but in 3 cases, it was able to indicate the correct MIC value of the compounds (1c, 4a and 4c, Table 2).

Table 2. Experimental and predicted MIC values (ug/mL) of the tested complexes against MRSA and MSSA *S. aureus* strains. The agreement between predicted and experimental MIC values (within x2 MIC) is indicated with a "yes/no" in the last two columns.

[†]Although not strictly within x2 MIC, we consider the prediction close enough to warrant agreement between predicted and experimental MIC values. * Indicates two diastereomeric forms of the same complex.

Species	Predicted MRSA	Predicted MSSA	Experiment MRSA	Experiment MSSA	Agreement MRSA	Agreement MSSA
1a	>32	19.4	>50	>50	yes	**no**
1b	>32	18.0	>50	>50	yes	**no**
1c	3.0	3.0	4.9	4.9	yes	**yes**
2a	10.1	5.1	>50	>50	no	**no**
2b	4.7	4.7	>50	>50	no	**no**
2c†	3.1	3.1	10.1	10.1	yes	**yes**
3a	>32	3.0	>50	>50	yes	**no**
3b	>32	2.9	>50	>50	yes	**no**
3c	>32	3.6	32	>50	yes	**no**
4a	17.5	17.5	13.6	13.6	yes	**yes**
4b	16.0	16.0	>50	>50	no	**no**
4c	11.1	5.6	12.5	6.3	yes	**yes**
5d	4.4	4.4	>8	8	no	**yes**
6d	4.4	4.4	8	8	yes	**yes**
7a	>32	>32	>32	>32	yes	**yes**
7b	>32	>32	>32	>32	yes	**yes**
8a	2.4	2.4	>50	>50	no	**no**
8d	4.1	4.1	8	8	yes	**yes**
8d*	4.1	4.1	8	8	yes	**yes**
9a	2.4	2.4	>50	>50	no	**no**
9d	4.1	4.1	8	8	yes	**yes**
9d*	**4.1**	**4.1**	**8**	**8**	**yes**	**yes**

Feature importance analysis

The effect of features and network architectures on the quality of the predictions was tested, and the distribution of the final scores for the features is presented in Figure 4. After evaluating the model performance, we examined the feature importance in the prediction model. The Neural Network is not a straightforward method to assess the intrinsic feature importance. For example, it is hard to interpret how these weights contribute to the resulting decisions just by analyzing the weights between the neurons in the model. The feature importance of the set of used descriptors was calculated based on their relative contributions to predictions made by the model. Below we try to assess the significance of feature j as follows:

$$f_j = s - \frac{1}{n}\sum_{i=1}^{n} s_{ij}$$

where s – is the baseline score computed for the non-permuted input data set; basically, it is equal to 1; sij – is the score obtained by permuting the corresponding feature column of the data set. By permuting, we mean that the values of the feature are randomly permuted between various data rows (molecules). In this way, the importance of a feature is the difference between the baseline score s and the average score obtained by permuting the corresponding column of the test set. If the difference is small, then the model is insensitive to permutations of the feature, so its importance is low. Conversely, the feature's importance is high if the difference is significant. The parameter n controls the number of permutations per feature — more permutations yield better estimates (we used n=100).

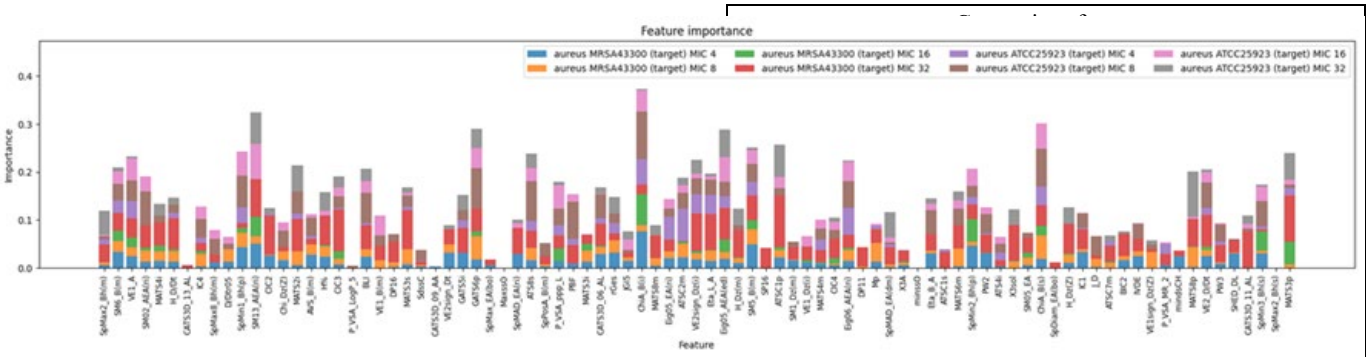

Figure 4. Molecular descriptor scoring.

This assessment with the low scores does not necessarily mean that the feature is not important at all but rather that most of its values are close to each other and possibly that when training. The top descriptor with the highest average effect in the prediction model is listed in Table 3. The Kier benzene-likeliness index (BLI) descriptors, which are calculated by dividing the first-order valence connectivity index by the number of non-H bonds (nBO) of the molecule and then normalizing on the benzene molecule proposed to measure the molecule aromaticity, were defined as a top-ranked feature of importance. This is true for all cases except the last case (*S. aureus* ATCC25923 (target) MIC 32).

Table 3. Top-scored descriptors for each of the target cases.

MRSA MIC 16	indices [28]	
S. aureus MRSA MIC 32	BLI - Topological indices [28]	
S. aureus MSSA MIC 4	BLI - Topological indices [28]	
S. aureus MSSA MIC 8	BLI - Topological indices [28]	
S. aureus MSSA MIC 16	BLI - Topological indices [28]	
S. aureus MSSA MIC 32	Edge adjacency indices [29]	Spectral moment of order 13 from augmented edge adjacency mat. weighted by resonance integral (structural properties of the graph)

A second method for the feature assessment was applied to investigate the effect and robustness of the obtained BLI descriptor as the top-ranked. The ranking was performed using Random Forest (RF, Bootstrap-aggregated (bagged) decision trees)[30], trained on a random forest of 200 classification trees, and stored the out-of-bag information for predictor importance estimation. The critical values are sorted and reported in the Excel file in the SI. Identical results were obtained with the RF. BLI aromaticity index was the top-ranked. The relationship between the antimicrobial activity and the impact of the BLI, indicates that the BLI is a crucial descriptor in the prediction models. The effect of the BLI descriptor could be connected to the lipophilicity of the molecules. Indeed, the solubility descriptor X3sol was detected, and it is also present in the list (SI) as one of the top-ranked descriptors. Other features of high relevance are edge adjacency indices (e.g., eigenvalue or spectral mean absolute deviation indices such as Eig05_EA (ri), Eig05_AEA (ed) or SpMAD_EA (dm) and SM13_AEA (ri)) derived from Graph.

The correlation between the hydrophobicity and antimicrobial activity was shown for the antimicrobial polymers. In this study [31], the logarithm of the partition coefficient of compounds between n-octanol (C logP) and water was used to represent hydrophobicity. The authors showed that the elevated responses from the antimicrobial activity required hydrophobicity that was neither too high nor too low. The obtained values suggest that C logP values between 0 and 2 have the best balance of high antimicrobial activity.

Then the obtained relations between the identified descriptors in the MLP model were explainable. The nature of the target should be tested as a limiting factor for the sparser application of the obtained results about the activity towards different bacterial cells. Still, it might display highly synergistic effects based on the selectivity of the descriptor. The defined descriptors (BLI and x3sol) could be used for designing the new antibacterial agents addressing different targets.

Conclusion

This study presents a model based on supervised learning methods to predict the antibacterial properties of Re-metals complexes. This machine-learning-guided descriptor model was developed on Re-metals complexes and was proven able to predict the antimicrobial activity of the metal complexes against the methicillin-resistant *S. aureus* ATCC 43300 strain with good accuracy and precision. It may thus serve as an advisory tool to guide the synthesis of new complexes. The MLP model makes use of (1) molecular representation based on the structure of the complexes, (2) feature reduction space, (3) ML algorithm, and (4) molecular descriptor specificity analysis (features *importance* scores). When applied to the prediction of 20 previously untested molecules, in 70% of cases, it was able to predict whether (a) the metal complex may be active or (b) inactive. Moreover, in >80% of correctly predicted active molecules, their minimum inhibitory concentration was predicted within 2x the experimentally determined values. The proposed ML-based antibiotic development approach revealed the main descriptors that are responsible for the antimicrobial activity. Therefore, the model may predict the activity of new unconventional antibacterial candidates based on Re-complexes with the selected molecular descriptors.

Materials and Methods

The Multi-layer Perceptron (MLP)[32] was used for the neural network model.

MLP is a supervised learning algorithm, the simplest kind of feed-forward network, as shown in Figure 5. In the architecture of the feed-forward neural networks, the units (or nodes) are arranged into a graph without any sequential loops. This contrasts with recurrent neural networks [33], where the graph can have loops, so the network feeds into itself from the loops. The MLP learns a function by training on a dataset and, consequently, the number of dimensions for input and the number of dimensions for output. It is different from logistic regression in that, between the input and the output layer, there can be one or more non-linear layers, called hidden layers. For the training of the model, MLP regressor trains using backpropagation with no activation function in the output layer, which can also be seen as using the identity function as an activation function. The model was trained on the provided data set having 119 data rows (input objects) s, 92 feature columns, and 2 output classes. This set was subdivided into 75% for the training set (89 data rows) and 25% for the validation set (30 data rows). The code used for the model, along with the training and test set provided in this repository: https://github.com/mici345/MIC-prediction-model

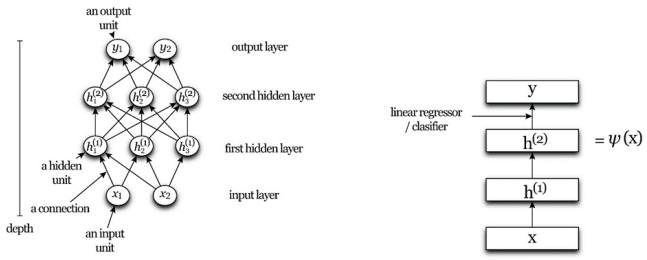

Figure 5. Multilayer perceptron with two hidden layers. Left picture: input layer, input features values are used for the input units. The output layer has one unit per each value of the network outputs. Hidden layers: the layers between in and out units. Right picture: layers presented as boxes.

Structure of the dataset, descriptors generation space, and descriptors importance

We initially used more than 5666 descriptors for building the model, which are representations of Re-compounds. The AlvaDesc software was used to generate descriptors space from the 3D structures of each Re-complex. The set of used descriptors includes 0D (with no relation to shape, e.g., molecular weight), 1D (e.g., presence of certain active substructures within the molecule), 2D (e.g., molecular graph representations involving bonds between atoms but not bond lengths), and 3D (e.g., distances between specific atomic pairs in the molecule) ones (details in the Supporting Information). The descriptors are likely to contain information which could be correlated to the antimicrobial action of a given Re-complex. The structure of the input matrix for the ML models often leads to decreasing predictive accuracy of the model. The reduction techniques are often performed to decrease the noise in data structure but at the same time the loss of information should be presumed. The data sets were reduced with Principal Component Analysis (PCA) for reducing the descriptor space. PCA is an orthogonal linear transformation that transforms the data into a new coordinate system where the first direction of the most significant variance becomes the new coordinate axis[36] . The optimal parameter selection within the descriptors space resulted in highly converged accuracies for the trained model. Construction of the initial matrix from the explored chemical database is a key feature for the development and validation of the model. The final reduced set was based on 119 data points (Re-complex), 91 feature , and 2 output classes for the bacterial strains.

Reagents and chemicals

All reagents were obtained from standard sources and utilized without any further purifications. The compounds $Re(CO)_5Cl$ was purchased from Sigma-Aldrich. For the validation set, complexes **1a** [37,38], **1b**[39], **1c** [40], **2a** [37,41], **2b** [42–44], **2c** [45], **3b** [46], **4b** [47,48], **7a** [37,49,50] and **7b** [43,44,51] were synthesized according to published procedures. Complexes **5d**, **6d**, **8d**, and **9d** were prepared according to Cortat *et al.*[1] Complexes **3a**, **3c**, **4a**, **4c**, **8a**, and **9a** were prepared with similar procedures. All complexes were synthesized under an inert (Ar) gas environment.

Instruments and Analysis

IR spectra were recorded on a Bruker TENSOR II with the following parameters: 16 scans for the background and 32 scans for the sample with a resolution of 4 cm^{-1} in the 4000 to 600 cm^{-1}

region. UV-Vis spectra of the complexes were measured on a Jasco V730 spectrophotometer. A Bruker Advance III 400 MHz was used to measure the complexes' NMR spectra. The corresponding ^{1}H chemical shifts were reported relative to. residual solvent protons. A Bruker FTMS 4.7-T Apex II in positive mode was used to perform the mass analyses.

Synthetic procedures

Ligands for complexes **2a-c** and **7a-b** were synthesized according to published procedures [52–56]. The $Re(CO)_5Br$ synthesis is detailed elsewhere [37,57,58]. For the preparation of the complexes in the validation set, $Re(CO)_5Br$ and $Re(CO)_5Cl$ were used. Rhenium precursors and ligands were generally reacted in equimolar ratios and refluxed overnight. After the reactions, products were filtered and washed with the reaction solvent and diethyl ether. The purity of the complexes (Br or Cl species **3a**, **4a**, **8a**, and **9a**) was confirmed as >95%. Compounds **3c** and **4c** were prepared by suspending **3a** or **4a** in MeOH (HPLC grade) with 1-mole equiv. of pyridine and AgOTf (1.2 mole equiv.) and refluxing in the dark overnight. After the mixture had cooled to room temperature, it was filtered to discard AgBr and dried in a vacuum oven. The compounds were then purified by HPLC. Spectrochemical characterization of the complexes are in the Supporting Information.

Antimicrobial study

The antimicrobial activity of $Re(CO)_3$ complexes was assessed against *S. aureus* ATCC 25923 (wild type, MSSA) and *S. aureus* ATCC 43300 (methicillin-resistant, MRSA) strains following published protocols [59,60]. Briefly, each complex was prepared as a 6.4 mM stock solution in DMSO and diluted to 256 µM with PBS. They were sterilized for 20 min under UV light before use. Then, stock samples were diluted with PBS to 128 µM, and 50 µL of each dilution was transferred to 96-well plates. In parallel, *S. aureus* in Mueller–Hinton Broth (non-cation-adjusted, MHB), cultured one-day before injection, was used to prepare bacterial suspensions at 1 x 10^6 CFU/mL in MHB 2X. Then, 50 µL of *S. aureus* suspensions were mixed in the 50 µL of serially diluted sample wells, leading to a final bacterial concentration of 5 x 10^5 and the complexes concentrations ranging from 64 µM to 0.5 µM. The plates were incubated at 37 °C for 24 h. The minimum inhibitory concentration (MIC) values were determined by measuring the optical density at 600 nm (OD600). The assay was conducted in triplicate. Tecan-Spark 10M with SparkControl program was used to determine the antimicrobial activities.

Supporting Information

The Supporting Information is available free of charge on the ACS Publications website.

Statistical metrics - Table S1 (file type, i.e., .xlsx)

Descriptors library - (file type, i.e., .xlsx)

Spectrochemical characterization of the complexes - (file type, i.e., .docx)

AUTHOR INFORMATION

Corresponding Author

Marco Lattuada - Department of Chemistry, Fribourg University, 1700 Fribourg, Switzerland

Authors

Miroslava Nedyalkova - Department of Chemistry, Fribourg University, 1700 Fribourg, Switzerland

Gözde Demirci - Department of Chemistry, Fribourg University, 1700 Fribourg, Switzerland

Youri Cortat - Department of Chemistry, Fribourg University, 1700 Fribourg, Switzerland

Kevin Schindler - Department of Chemistry, Fribourg University, 1700 Fribourg, Switzerland

Fatlinda Rhamani - Department of Chemistry, Fribourg University, 1700 Fribourg, Switzerland

Aleksandar Pavic-Institute of Molecular Genetics and Genetic Engineering, University of Belgrade, 11042 Belgrade, Serbia

Fabio Zobi- Department of Chemistry, Fribourg University, 1700 Fribourg, Switzerland

Author Contributions

M.N., F.Z., and M.L. designed the project., M.N. performed the computational study. G.D. performed antimicrobial and experimental studies. Y.C .and, K.S. and F.R. - experimental, A.P. antimicrobial testing, M.N., F.Z., and M.L.-original draft, writing-review& editing

ACKNOWLEDGMENT

The work was supported by Swiss National Science Foundation, NCCR Bioinspired Materials

REFERENCES

(1) Cortat, Y.; Nedyalkova, M.; Schindler, K.; Kadakia, P.; Demirci, G.; Nasiri Sovari, S.; Crochet, A.; Salentinig, S.; Lattuada, M.; Steiner, O. M.; Zobi, F. Computer-Aided Drug Design and Synthesis of Rhenium Clotrimazole Antimicrobial Agents. Antibiotics 2023, 12 (3), 619. https://doi.org/10.3390/antibiotics12030619.

(2) Cooper, S. M.; Siakalli, C.; White, A. J. P.; Frei, A.; Miller, P. W.; Long, N. J. Synthesis and Anti-Microbial Activity of a New Series of Bis(Diphosphine) Rhenium(<scp>v</Scp>) Dioxo Complexes. Dalton Transactions 2022, 51 (34), 12791–12795. https://doi.org/10.1039/D2DT02157A.

(3) Frei, A.; Amado, M.; Cooper, M. A.; Blaskovich, M. A. T. Light-Activated Rhenium Complexes with Dual Mode of Action against Bacteria. Chemistry – A European Journal 2020, 26 (13), 2852–2858. https://doi.org/10.1002/chem.201904689.

(4) Sovari, S. N.; Radakovic, N.; Roch, P.; Crochet, A.; Pavic, A.; Zobi, F. Combatting AMR: A Molecular Approach to the Discovery of Potent and Non-Toxic Rhenium Complexes Active against C. Albicans-MRSA Co-Infection. Eur J Med Chem 2021, 226, 113858. https://doi.org/10.1016/j.ejmech.2021.113858.

(5) Sovari, S. N.; Vojnovic, S.; Bogojevic, S. S.; Crochet, A.; Pavic, A.; Nikodinovic-Runic, J.; Zobi, F. Design, Synthesis and in Vivo Evaluation of 3-Arylcoumarin Derivatives of Rhenium(I) Tricarbonyl Complexes as Potent Antibacterial Agents against Methicillin-Resistant Staphylococcus Aureus (MRSA). Eur J Med Chem 2020, 205, 112533. https://doi.org/10.1016/j.ejmech.2020.112533.

(6) Slate, A. J.; Shalamanova, L.; Akhidime, I. D.; Whitehead, K. A. Rhenium and Yttrium Ions as Antimicrobial Agents against Multidrug Resistant Klebsiella Pneumoniae and Acinetobacter Baumannii Biofilms. Lett Appl Microbiol 2019, lam.13154. https://doi.org/10.1111/lam.13154.

(7) Siegmund, D.; Lorenz, N.; Gothe, Y.; Spies, C.; Geissler, B.; Prochnow, P.; Nuernberger, P.; Bandow, J. E.; Metzler-Nolte, N. Benzannulated Re(<scp>i</Scp>)–NHC Complexes: Synthesis, Photophysical Properties and Antimicrobial Activity. Dalton Transactions 2017, 46 (44), 15269–15279. https://doi.org/10.1039/C7DT02874A.

(8) Patra, M.; Wenzel, M.; Prochnow, P.; Pierroz, V.; Gasser, G.; Bandow, J. E.; Metzler-Nolte, N. An Organometallic Structure-Activity Relationship Study Reveals the Essential Role of a Re(CO) 3 Moiety in the Activity against Gram-Positive Pathogens Including MRSA. Chem Sci 2015, 6 (1), 214–224. https://doi.org/10.1039/C4SC02709D.

(9) Wenzel, M.; Patra, M.; Senges, C. H. R.; Ott, I.; Stepanek, J. J.; Pinto, A.; Prochnow, P.; Vuong, C.; Langklotz, S.; Metzler-Nolte, N.; Bandow, J. E. Analysis of the Mechanism of Action of Potent Antibacterial Hetero-Tri-Organometallic Compounds: A Structurally New Class of Antibiotics. ACS Chem Biol 2013, 8 (7), 1442–1450. https://doi.org/10.1021/cb4000844.

(10) Mendes, S. S.; Marques, J.; Mesterházy, E.; Straetener, J.; Arts, M.; Pissarro, T.; Reginold, J.; Berscheid, A.; Bornikoel, J.; Kluj, R. M.; Mayer, C.; Oesterhelt, F.; Friães, S.; Royo, B.; Schneider, T.; Brötz-Oesterhelt, H.; Romão, C. C.; Saraiva, L. M. Synergetic Antimicrobial Activity and Mechanism of Clotrimazole-Linked CO-Releasing Molecules. ACS Bio & Med Chem Au 2022, 2 (4), 419–436. https://doi.org/10.1021/acsbiomedchemau.2c00007.

(11) Schindler, K.; Cortat, Y.; Nedyalkova, M.; Crochet, A.; Lattuada, M.; Pavic, A.; Zobi, F. Antimicrobial Activity of Rhenium Di- and Tricarbonyl Diimine Complexes: Insights on Membrane-Bound S. Aureus Protein Binding. Pharmaceuticals 2022, 15 (9), 1107. https://doi.org/10.3390/ph15091107.

(12) Camacho, D. M.; Collins, K. M.; Powers, R. K.; Costello, J. C.; Collins, J. J. Next-Generation Machine Learning for Biological Networks. Cell 2018, 173 (7), 1581–1592. https://doi.org/10.1016/j.cell.2018.05.015.

(13) Vakarelska, E.; Nedyalkova, M.; Vasighi, M.; Simeonov, V. Persistent Organic Pollutants (POPs) - QSPR Classification Models by Means of Machine Learning Strategies. Chemosphere 2022, 287, 132189. https://doi.org/10.1016/j.chemosphere.2021.132189.

(14) Souza, M. C. O.; Cruz, J. C.; Rocha, B. A.; Souza, J. M. O.; Devóz, P. P.; Santana, A.; Campíglia, A. D.; Barbosa, F. The Influence of the Co-Exposure to Polycyclic Aromatic Hydrocarbons and Toxic Metals on DNA Damage in Brazilian Lactating Women and Their Infants: A Cross-Sectional Study Using Machine Learning Approaches. Chemosphere 2023, 334, 138975. https://doi.org/10.1016/j.chemosphere.2023.138975.

(15) Chatterjee, M.; Roy, K. Chemical Similarity and Machine Learning-Based Approaches for the Prediction of Aquatic Toxicity of Binary and Multicomponent Pharmaceutical and Pesticide Mixtures against Aliivibrio Fischeri. Chemosphere 2022, 308, 136463. https://doi.org/10.1016/j.chemosphere.2022.136463.

(16) Gajewicz-Skretna, A.; Furuhama, A.; Yamamoto, H.; Suzuki, N. Generating Accurate in Silico Predictions of Acute Aquatic Toxicity for a Range of Organic Chemicals: Towards Similarity-Based Machine Learning Methods. Chemosphere 2021, 280, 130681. https://doi.org/10.1016/j.chemosphere.2021.130681.

(17) Ruiz Puentes, P.; Henao, M. C.; Cifuentes, J.; Muñoz-Camargo, C.; Reyes, L. H.; Cruz, J. C.; Arbeláez, P. Rational Discovery of Antimicrobial Peptides by Means of Artificial Intelligence. Membranes (Basel) 2022, 12 (7), 708. https://doi.org/10.3390/membranes12070708.

(18) Ren, Y.; Chakraborty, T.; Doijad, S.; Falgenhauer, L.; Falgenhauer, J.; Goesmann, A.; Hauschild, A.-C.; Schwengers, O.; Heider, D. Prediction of Antimicrobial Resistance Based on Whole-Genome Sequencing and Machine Learning. Bioinformatics 2022, 38 (2), 325–334. https://doi.org/10.1093/bioinformatics/btab681.

(19) Huang, Y.; Sheth, R. U.; Zhao, S.; Cohen, L. A.; Dabaghi, K.; Moody, T.; Sun, Y.; Ricaurte, D.; Richardson, M.; Velez-Cortes, F.; Blazejewski, T.; Kaufman, A.; Ronda, C.; Wang, H. H. High-Throughput Microbial Culturomics Using Automation and Machine Learning. Nat Biotechnol 2023. https://doi.org/10.1038/s41587-023-01674-2.

(20) Skinnider, M. A.; Johnston, C. W.; Gunabalasingam, M.; Merwin, N. J.; Kieliszek, A. M.; MacLellan, R. J.; Li, H.; Ranieri, M. R. M.; Webster, A. L. H.; Cao, M. P. T.; Pfeifle, A.; Spencer, N.; To, Q. H.; Wallace, D. P.; Dejong, C. A.; Magarvey, N. A. Comprehensive Prediction of Secondary Metabolite Structure and Biological Activity from Microbial Genome Sequences. Nat Commun 2020, 11 (1), 6058. https://doi.org/10.1038/s41467-020-19986-1.

(21) Durrant, J. D.; Amaro, R. E. Machine-Learning Techniques Applied to Antibacterial Drug Discovery. Chem Biol Drug Des 2015, 85 (1), 14–21. https://doi.org/10.1111/cbdd.12423.

(22) Martin, E. J.; Polyakov, V. R.; Zhu, X.-W.; Tian, L.; Mukherjee, P.; Liu, X. All-Assay-Max2 PQSAR: Activity Predictions as Accurate as Four-Concentration IC 50 s for 8558 Novartis Assays. J Chem Inf Model 2019, 59 (10), 4450–4459. https://doi.org/10.1021/acs.jcim.9b00375.

(23) Tiihonen, A.; Cox-Vazquez, S. J.; Liang, Q.; Ragab, M.; Ren, Z.; Hartono, N. T. P.; Liu, Z.; Sun, S.; Zhou, C.; Incandela, N. C.; Limwongyut, J.; Moreland, A. S.; Jayavelu, S.; Bazan, G. C.; Buonassisi, T. Predicting Antimicrobial Activity of Conjugated Oligoelectrolyte Molecules via Machine Learning. J Am Chem Soc 2021, 143 (45), 18917–18931. https://doi.org/10.1021/jacs.1c05055.

(24) Medvedeva, A.; Teimouri, H.; Kolomeisky, A. B. Predicting Antimicrobial Activity for Untested Peptide-Based Drugs Using Collaborative Filtering and Link Prediction. J Chem Inf Model 2023, 63 (12), 3697–3704. https://doi.org/10.1021/acs.jcim.3c00137.

(25) Ishfaq, M.; Aamir, M.; Ahmad, F.; M Mebed, A.; Elshahat, S. Machine Learning-Assisted Prediction of the Biological Activity of Aromatase Inhibitors and Data Mining to Explore Similar Compounds. ACS Omega 2022, 7 (51), 48139–48149. https://doi.org/10.1021/acsomega.2c06174.

(26) Diéguez-Santana, K.; González-Díaz, H. Machine Learning in Antibacterial Discovery and Development: A Bibliometric and Network Analysis of Research Hotspots and Trends. Comput Biol Med 2023, 155, 106638. https://doi.org/10.1016/j.compbiomed.2023.106638.

(27) Frei, A.; Elliott, A. G.; Kan, A.; Dinh, H.; Bräse, S.; Bruce, A. E.; Bruce, M. R.; Chen, F.; Humaidy, D.; Jung, N.; King, A. P.; Lye, P. G.; Maliszewska, H. K.; Mansour, A. M.; Matiadis, D.; Muñoz, M. P.; Pai, T.-Y.; Pokhrel, S.; Sadler, P. J.; Sagnou, M.;

Taylor, M.; Wilson, J. J.; Woods, D.; Zuegg, J.; Meyer, W.; Cain, A. K.; Cooper, M. A.; Blaskovich, M. A. T. Metal Complexes as Antifungals? From a Crowd-Sourced Compound Library to the First In Vivo Experiments. JACS Au 2022, 2 (10), 2277–2294. https://doi.org/10.1021/jacsau.2c00308.

(28) Basak, S. C.; Balaban, A. T.; Grunwald, G. D.; Gute, B. D. Topological Indices: Their Nature and Mutual Relatedness. J Chem Inf Comput Sci 2000, 40 (4), 891–898. https://doi.org/10.1021/ci990114y.

(29) Todeschini, R.; Consonni, V. Molecular Descriptors for Chemoinformatics; Wiley, 2009. https://doi.org/10.1002/9783527628766.

(30) Tin Kam Ho. Random Decision Forests. In Proceedings of 3rd International Conference on Document Analysis and Recognition; IEEE Comput. Soc. Press; pp 278–282. https://doi.org/10.1109/ICDAR.1995.598994.

(31) Phuong, P. T.; Oliver, S.; He, J.; Wong, E. H. H.; Mathers, R. T.; Boyer, C. Effect of Hydrophobic Groups on Antimicrobial and Hemolytic Activity: Developing a Predictive Tool for Ternary Antimicrobial Polymers. Biomacromolecules 2020, 21 (12), 5241–5255. https://doi.org/10.1021/acs.biomac.0c01320.

(32) Haykin, S. Neural Networks: A Comprehensive Foundation. ; 1994.

(33) Schmidt, R. M. Recurrent Neural Networks (RNNs): A Gentle Introduction and Overview. 2019.

(34) Mauri, A. AlvaDesc: A Tool to Calculate and Analyze Molecular Descriptors and Fingerprints; 2020; pp 801–820. https://doi.org/10.1007/978-1-0716-0150-1_32.

(35) Mauri, A.; Bertola, M. Alvascience: A New Software Suite for the QSAR Workflow Applied to the Blood–Brain Barrier Permeability. Int J Mol Sci 2022, 23 (21), 12882. https://doi.org/10.3390/ijms232112882.

(36) Kruskal, J. B. Nonmetric Multidimensional Scaling: A Numerical Method. Psychometrika 1964, 29 (2), 115–129. https://doi.org/10.1007/BF02289694.

(37) Kurz, P.; Probst, B.; Spingler, B.; Alberto, R. Ligand Variations in [ReX(Diimine)(CO) 3] Complexes: Effects on Photocatalytic CO 2 Reduction. Eur J Inorg Chem 2006, 2006 (15), 2966–2974. https://doi.org/10.1002/ejic.200600166.

(38) Moya, S. A.; Guerrero, J.; Pastene, R.; Schmidt, R.; Sariego, R.; Sartori, R.; Sanz-Aparicio, J.; Fonseca, I.; Martinez-Ripoll, M. Metallic Carbonyl Compleies Containing Heterocycle Nitrogen Ligands. 2. Tricarbonylbromo(3,3'-R-2,2'-Biquinoline)Rhenium(I) Compounds; 1994; Vol. 33. https://pubs.acs.org/sharingguidelines.

(39) Machura, B.; Kruszynski, R.; Kusz, J. X-Ray Structure, Spectroscopic Characterisation and DFT Calculations of the [Re(CO)3(Dppt)Cl] Complex. Polyhedron 2007, 26 (8), 1590–1596. https://doi.org/10.1016/j.poly.2006.11.034.

(40) Moya, S. A.; Guerrero, J.; Rodriguez-Nieto, F. J.; Wolcan, E.; Féliz, M. R.; Baggio, R. F.; Garland, M. T. Influence of the 4-Substituted Pyridine Ligand L′ on Both the Conformation and Spectroscopic Properties of the (2,2′-Biquinoline-KN1,KN1′)Tricarbonyl(Pyridine-KN1)Rhenium(1+) Complex ([Re(CO)3-(Bqui)(Py)]+) and Its Derivatives [Re(CO)3(L)(L′)]+ (L = 2,2′-Biquinoline and 3,3′-(Ethane-1,2-Diyl)-2,2′-Biquinoline). Helv Chim Acta 2005, 88 (11), 2842–2860. https://doi.org/10.1002/hlca.200590227.

(41) Liang, Y.; Nguyen, M. T.; Holliday, B. J.; Jones, R. A. Electrocatalytic Reduction of CO2 Using Rhenium Complexes with Dipyrido[3,2-a:2′,3′-c]Phenazine Ligands. Inorg Chem Commun 2017, 84, 113–117. https://doi.org/10.1016/j.inoche.2017.08.002.

(42) Sousa, S. F.; Sampaio, R. N.; Barbosa Neto, N. M.; Machado, A. E. H.; Patrocinio, A. O. T. The Photophysics of Fac-[Re(CO)3(NN)(Bpa)]+ Complexes: A Theoretical/Experimental Study. Photochemical & Photobiological Sciences 2014, 13 (8), 1213–1224. https://doi.org/10.1039/c4pp00074a.

(43) Stoeffler, H. D.; Thornton, N. B.; Temkin, S. L.; Schanze, K. S. Unusual Photophysics of a Rhenium(I) Dipyridophenazine Complex in Homogenous Solution and Bound to DNA; 1995; Vol. 117. https://pubs.acs.org/sharingguidelines.

(44) Ruiz, G. T.; Juliarena, M. P.; Lezna, R. O.; Wolcan, E.; Feliz, M. R.; Ferraudi, G. Intercalation of Fac-[(4,4′-Bpy)Re I (CO) 3 (Dppz)] + , Dppz = Dipyridyl[3,2-a:2′3′-c]Phenazine, in Polynucleotides. On the UV-Vis Photophysics of the Re(<scp>i</Scp>) Intercalator and the Redox Reactions with Pulse Radiolysis-Generated Radicals. Dalton Trans. 2007, No. 20, 2020–2029. https://doi.org/10.1039/B614970G.

(45) Wing-Wah Yam, V.; Kam-Wing Lo, K.; Cheung, K.-K.; Yuen-Chong Kong, R. Deoxyribonucleic Acid Binding and Photocleavage Studies of Rhenium(I) Dipyridophenazine Complexes. Journal of the Chemical Society, Dalton Transactions 1997, No. 12, 2067–2072. https://doi.org/10.1039/a700828g.

(46) Klein, D. M.; Rodríguez-Jiménez, S.; Hoefnagel, M. E.; Pannwitz, A.; Prabhakaran, A.; Siegler, M. A.; Keyes, T. E.; Reisner, E.; Brouwer, A. M.; Bonnet, S. Shorter Alkyl Chains Enhance Molecular Diffusion and Electron Transfer Kinetics between Photosensitisers and Catalysts in CO 2 -Reducing Photocatalytic Liposomes. Chemistry – A European Journal 2021, 27 (68), 17203–17212. https://doi.org/10.1002/chem.202102989.

(47) Sinha, S.; Berdichevsky, E. K.; Warren, J. J. Electrocatalytic CO 2 Reduction Using Rhenium(I) Complexes with Modified 2-(2′-Pyridyl)Imidazole Ligands. Inorganica Chim Acta 2017, 460, 63–68. https://doi.org/10.1016/j.ica.2016.09.019.

(48) Tzeng, B.-C.; Chen, B.-S.; Chen, C.-K.; Chang, Y.-P.; Tzeng, W.-C.; Lin, T.-Y.; Lee, G.-H.; Chou, P.-T.; Fu, Y.-J.; Chang, A. H.-H. PH-Dependent Spectroscopic and Luminescent Properties, and Metal-Ion Recognition Studies of Re(I) Complexes Containing 2-(2′-Pyridyl)Benzimidazole and 2-(2′-Pyridyl)Benzimidazolate. Inorg Chem 2011, 50 (12), 5379–5388. https://doi.org/10.1021/ic1019058.

(49) Carreño, A.; Aros, A. E.; Otero, C.; Polanco, R.; Gacitúa, M.; Arratia-Pérez, R.; Fuentes, J. A. Substituted Bidentate and Ancillary Ligands Modulate the Bioimaging Properties of the Classical Re(<scp>i</Scp>) Tricarbonyl Core with Yeasts and Bacteria. New Journal of Chemistry 2017, 41 (5), 2140–2147. https://doi.org/10.1039/C6NJ03792E.

(50) Bortoluzzi, M.; Battistel, D.; Albertin, G.; Daniele, S.; Enrichi, F.; Rumonato, R. Mononuclear and Heterodinuclear Phenanthrolinedione Complexes of D- and f-Block Elements‡. Chemical Papers 2016, 70 (1). https://doi.org/10.1515/chempap-2015-0140.

(51) Kaplanis, M.; Stamatakis, G.; Papakonstantinou, V. D.; Paravatou-Petsotas, M.; Demopoulos, C. A.; Mitsopoulou, C. A. Re(I) Tricarbonyl Complex of 1,10-Phenanthroline-5,6-Dione: DNA Binding, Cytotoxicity, Anti-Inflammatory and Anti-Coagulant Effects towards Platelet Activating Factor. J Inorg Biochem 2014, 135, 1–9. https://doi.org/10.1016/j.jinorgbio.2014.02.003.

(52) Dickeson, J.; Summers, L. Derivatives of 1,10-Phenanthroline-5,6-Quinone. Aust J Chem 1970, 23 (5), 1023. https://doi.org/10.1071/CH9701023.

(53) Molphy, Z.; Prisecaru, A.; Slator, C.; Barron, N.; McCann, M.; Colleran, J.; Chandran, D.; Gathergood, N.; Kellett, A. Copper Phenanthrene Oxidative Chemical Nucleases. Inorg Chem 2014, 53 (10), 5392–5404. https://doi.org/10.1021/ic500914j.

(54) Greguric, A.; Greguric, I. D.; Hambley, T. W.; Aldrich-Wright, J. R.; Collins, J. G. Minor Groove Intercalation of Δ-[Ru(Me2phen)2dppz]2+ to the Hexanucleotide d(GTCGAC)2. Journal of the Chemical Society, Dalton Transactions 2002, No. 6, 849. https://doi.org/10.1039/b105689c.

(55) Wang, C.; Lystrom, L.; Yin, H.; Hetu, M.; Kilina, S.; McFarland, S. A.; Sun, W. Increasing the Triplet Lifetime and Extending the Ground-State Absorption of Biscyclometalated Ir(<scp>iii</Scp>) Complexes for Reverse Saturable Absorption and Photodynamic Therapy Applications. Dalton Transactions 2016, 45 (41), 16366–16378. https://doi.org/10.1039/C6DT02416E.

(56) Nagaraj, K.; Senthil Murugan, K.; Thangamuniyandi, P.; Sakthinathan, S. Synthesis, Micellization Behaviour, DNA/RNA Binding and Biological Studies of a Surfactant Cobalt(III) Complex With Dipyrido[3,2-a:2′,4′-c](6,7,8,9-Tetrahydro)Phenazine. J Fluoresc 2014, 24 (6), 1701–1714. https://doi.org/10.1007/s10895-014-1457-1.

(57) Sovari, S. N.; Radakovic, N.; Roch, P.; Crochet, A.; Pavic, A.; Zobi, F. Combatting AMR: A Molecular Approach to the Discovery of Potent and Non-Toxic Rhenium Complexes Active against C. Albicans-MRSA Co-Infection. Eur J Med Chem 2021, 226, 113858. https://doi.org/10.1016/j.ejmech.2021.113858.

(58) Schmidt, S. P. Pentacarbonylrhenium Halides. . In Inorganic syntheses: Reagents for transition metal complex organometallic syntheses; 1990; Vol. 28, pp 160–165.

(59) Barry, A. L. Methods for Determining Bactericidal Activity of Antimicrobial Agents: Approved Guideline. In National Committee for Clinical Laboratory Standards; 1999; Vol. 19.

(60) Wiegand, I.; Hilpert, K.; Hancock, R. E. W. Agar and Broth Dilution Methods to Determine the Minimal Inhibitory Concentration (MIC) of Antimicrobial Substances. Nat Protoc 2008, 3 (2), 163–175. https://doi.org/10.1038/nprot.2007.521.

SYNOPSIS TOC (Word Style “SN_Synopsis_TOC”). If you are submitting your paper to a journal that requires a synopsis graphic and/or synopsis paragraph, see the Instructions for Authors on the journal’s homepage for a description of what needs to be provided and for the size requirements of the artwork.